Hindawi
Geofluids
Volume 2020, Article ID 5702031, 11 pages
https://doi.org/10.1155/2020/5702031

Research Article

Geochemical Characteristics and Productivity Response of Produced Water from Coalbed Methane Wells in the Yuwang Block, Eastern Yunnan, China

Mingyang Du,[1,2] Xiaojuan Yao,[1,2] Shasha Zhang,[1,2] He Zhou,[1,2] Caifang Wu,[1,2] and Junlong Zhao[1,2]

[1]*Key Laboratory of Coalbed Methane Resource and Reservoir Formation Process, Ministry of Education, Xuzhou, Jiangsu 221006, China*
[2]*School of Resources and Geoscience, China University of Mining and Technology, Xuzhou, Jiangsu 221006, China*

Correspondence should be addressed to Caifang Wu; caifangwu@126.com

Received 17 January 2020; Accepted 27 April 2020; Published 25 May 2020

Academic Editor: Jean-Luc Michelot

Coalbed methane (CBM) well-produced water contains abundant geochemical information that can guide productivity predictions of CBM wells. The geochemical characteristics and productivity responses of water produced from six CBM wells in the Yuwang block, eastern Yunnan, were analyzed using data of conventional ions, hydrogen and oxygen isotopes, and dissolved inorganic carbon (DIC). The results showed that the produced water type of well L-3 is mainly Na-HCO_3, while those from the other five wells are Na-Cl-HCO_3. The isotope characteristics of produced water are affected greatly by water-rock interaction. Combined with the enrichment mechanisms of isotopes D and ^{18}O, we found that the water samples exhibit an obvious D drift trend relative to the local meteoric water line. The ^{13}C enrichment of DIC in the water samples suggests that DIC is mainly produced by the dissolution of carbonate minerals in coal seams. The concentration of HCO_3^-, D drift trend, and enrichment of $^{13}C_{DIC}$ in produced water are positively correlated with CBM production, which can be verified by wells L-4 and L-6.

1. Introduction

Coalbed methane (CBM) is an unconventional natural gas resource, which has huge reserves worldwide [1–3]. The East of Yunnan and the West of Guizhou are important CBM resource areas in South China [4]. CBM production is achieved through drainage and reductions in pressure. Water discharged in this process undergoes various physical, chemical, and biological interactions with coal seams and surrounding rocks during the continuous runoff process, resulting in changes to the chemical composition and properties of the produced water [5–9]. Previous studies have shown that CBM well drainage water from all over the world has similar ion characteristics despite highly variant conditions (chemical composition, coal structure, coal metamorphic degree, study area, the original water source, and formation time): the concentrations of Na^+, K^+, and Cl^- are high, and the concentrations of Ca^{2+}, Mg^{2+}, and SO_4^{2-} are low [2, 10–14]. Researchers generally believe that the high concentrations of Na^+, K^+, and Cl^- in CBM well water in the early stage are caused by pollution from fracturing fluids used to open the coal seam [15, 16]. Produced water from CBM wells exhibits distinct geochemical characteristics at different drainage stages. With the development of drainage, the quality of water produced from CBM wells can be divided into three stages: fracturing fluid flowback, transitional, and stabilization. The corresponding water quality types are Na-Cl, Na-Cl-HCO_3, and Na-HCO_3, respectively [17–20].

H and ^{16}O isotopes in the formation water can be replaced with D and ^{18}O isotopes in the coal seam and surrounding rock, resulting in the increase of D and ^{18}O isotopes in the coal seam water in the reduction environment of coal measures [21, 22]. In addition, microorganisms can produce HDS, which is soluble in water and can exchange isotopes, leading to D drift characteristics of formation water in a sealed and reduced coal seam environment [21, 23–26].

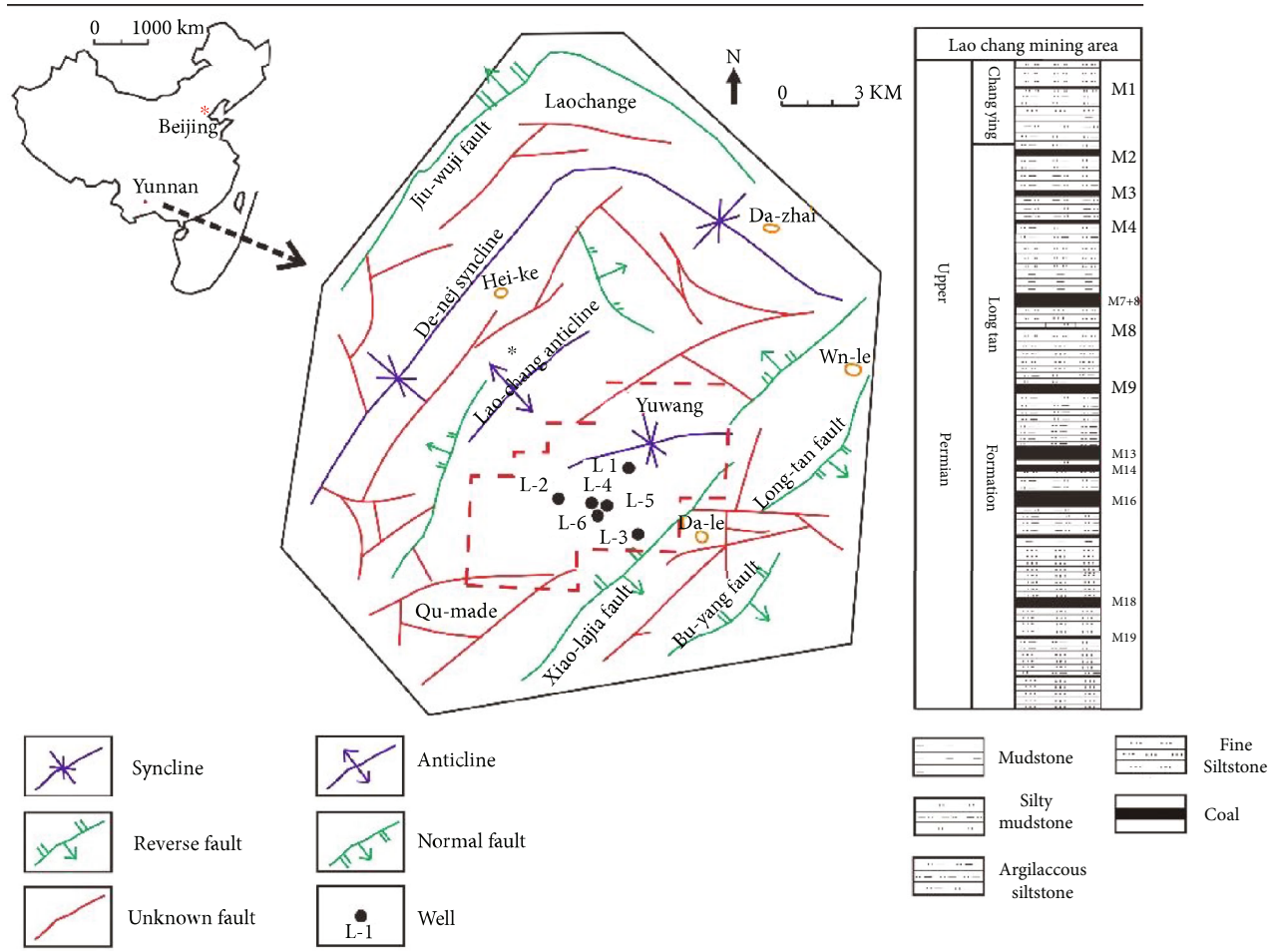

Figure 1: Study area structure and map of well locations.

There are significant differences in the composition of dissolved inorganic carbon isotopes ($^{13}C_{DIC}$) from various sources. Only a few studies have examined the dissolved inorganic carbon (DIC) in the produced water; these found that the $\delta^{13}C_{DIC}$ value for the decomposition of organic matter is less than -8‰, which is typical. The value of $\delta^{13}C_{DIC}$ released by carbonate dissolution or metamorphism is relatively high, and it is generally distributed around 0‰ [27–29].

The higher the concentration of HCO_3^- in CBM well water, the higher the gas content and productivity of the CBM wells [18, 30, 31]. It is suggested that the reason for the higher HCO_3^- content in high-level CBM wells may be the result of CO_2 migration and dissolution from low to high portions of CBM [23]. The distribution characteristics of hydrogen and oxygen isotopes in the produced water of CBM are related to the change of groundwater environment, which can be used as an index to judge the characteristics of groundwater and the productivity response of CBM wells [16, 32]. Based on the analysis of $^{13}C_{DIC}$ from different sources, it is generally believed that the decrease of methanogenic bacteria can lead to the abnormally positive characteristic of $^{13}C_{DIC}$ [27–29, 33–35].

Previous examinations of the geochemical characteristics of water produced by CBM wells have primarily been focused on the Qinshui Basin, Ordos Basin, and Guizhou Province in China [15, 32]. There are few reports on the geochemical characteristics of water produced by CBM wells in eastern Yunnan. Based on the test results of conventional ions, hydrogen and oxygen isotopes, and DIC of water samples from six CBM wells in the Yuwang block of eastern Yunnan in 2018, this study systematically analyzed the geochemical characteristics of the produced water and its significance for well productivity. It could provide a theoretical basis for CBM exploration and development in eastern Yunnan.

2. Geological Background and Materials

2.1. Geological Background. The Yuwang block is located near Qujing City, Fuyuan County, and is within the Laochang anticline structural belt on the southwestern margin of the Yangtze quasi-platform. The faults in the block are primarily NE-trending, with NW-trending transverse faults and NW-trending arc faults primarily distributed on the margins of the block. Most of the faults with an elevation decrease of greater than 100 m are boundary faults, while internal faults are scarce and mostly distributed near the folds (Figure 1). The main coal-bearing stratum is the Upper Permian Longtan Formation, with a thickness of 415–475 m. The main coal

Table 1: Characteristics of production wells.

CBM wells	Water production date	Main coal seam	Depth (m)	Average daily gas production (m^3)	Cumulative gas production (m^3)	Cumulative water production (m^3)
L-1	Apr. 2018	7+8/13	780.00	171.72	15787.22	258.31
L-2	Apr. 2018	16/18/19	735.60	219.97	21983.67	341.15
L-3	May 2018	13/14/19	832.00	34.54	1067.21	1575.76
L-4	May 2018	13/16/18/19	713.20	324.06	18762.31	404.54
L-5	May 2018	13/19	789.20	56.73	2886.88	254.12
L-6	May 2018	14/16/18	745.80	220.19	11864.53	322.25

seams are Nos. 3, 7+8, 16, 17+18, and 23. The coal in the study area ranks as anthracite; the maximum Ro value is between 2.53 and 3.50%, with an average of 2.99%. Methanogenesis ends at the medium volatile bituminous coal stage [33]. Therefore, the formation of coalbed methane is due to thermogenic rather than biogenic processes, and the methanogenesis is very weak in the study area. The petrographic composition of coal in the area is primarily semidark to semibright. This area is in the watersheds of the Huangni River, Xijiuxi River, and Seyi River, with a high terrain and an undeveloped surface water system.

There are six CBM development test wells (wells L-1, L-2, L-3, L-4, L-5, and L-6) that adopted the "segmented fracturing, combined layer drainage" developmental mode in the Yuwang block. Wells L-1 and L-2 began producing water from April 2018, while wells L-3, L-4, L-5, and L-6 began producing water in May 2018. The cumulative water and gas production of the six wells by November 2018 can be seen in Table 1. Well L-2 produced the most gas (21983.67 m^3) during this period, followed by wells L-4, L-1, L-6, L-5, and L-3. Well L-3 had the highest cumulative water production, at 1575.76 m^3, followed by wells L-4, L-2, L-6, L-1, and L-5.

2.2. Samples. Since April 2018, water samples from six wells in the Yuwang block have been collected and tested. Water was sampled directly from the wellhead in 2.5 L pure water bottles, rinsed a minimum of three times with the produced water sample. Samples were then sent to the Institute of Geochemistry, Guiyang Academy of Sciences, for relevant content analysis within 72 h. The experimental content includes conventional anion and cation mass concentration tests, hydrogen and oxygen stable isotope tests, and a DIC test. As of November 2018, 37 samples had been collected from the six wells (Table 2).

3. Results and Discussion

3.1. Conventional Ion Characteristics and Productivity Response. The produced water from six CBM wells in the study area exhibited similar characteristics: the Na^+, Cl^-, and HCO_3^- concentrations were relatively high, those of Ca^{2+}, Mg^{2+}, and SO_4^{2-} were relatively low, and that of K^+ was between these two extremes (Table 2). Moreover, the concentration value of SO_4^{2-} in wells L-4, L-5, and L-6 was lower than that in the other wells. With the development of drainage, water produced from well L-3 in the study area shifted from the Na-Cl-HCO_3 type to the Na-HCO_3 type, while that from the other five wells were all characterized as Na-Cl-HCO_3 type. The conventional ion concentrations of K^+, Na^+, Ca^{2+}, Mg^{2+}, Cl^-, and SO_4^{2-} in the produced water from the six wells exhibited a fluctuating but ultimately decreasing trend, while the concentration of HCO_3^- presented a trend of increasing fluctuations (Figures 2(a)–2(g)). Among these ions, the concentrations of K^+, Na^+, Ca^{2+}, Mg^{2+}, Cl^-, and SO_4^{2-} in wells L-1 and L-2 varied greatly with time. The concentrations of K^+, Na^+, and Cl^- in wells L-3, L-4, L-5, and L-6 tended to stabilize with time while the concentrations of Ca^{2+}, Mg^{2+}, and SO_4^{2-} in those wells tended to fluctuate with time.

The ion characteristics in produced water in this study were similar to those of CBM wells in other areas [10, 11, 23]. Researchers generally hypothesize that the concentrations of Na^+, K^+, Cl^-, and HCO_3^- in coal seam water are low. However, the concentrations of Na^+, K^+, and Cl^- in water contaminated by fracturing fluid are greatly increased, while the concentration of HCO_3^- is reduced and the concentrations of other ions are less impacted. The concentrations of Na^+, K^+, Cl^-, and HCO_3^- in surface water are low, but the concentrations of Ca^{2+}, Mg^{2+}, and SO_4^{2-} are higher than those in the coal seam water [15, 16].

Generally, a closed groundwater environment is conducive to the enrichment and preservation of CBM while an open groundwater environment is not. Researchers theorize that open hydrological environments are close to oxygen-rich water source recharge areas that can enrich Ca^{2+}, Mg^{2+}, and SO_4^{2-}, while closed hydrological environments are far from such recharge areas and exhibit Na^+, K^+, Cl^-, and HCO_3^- enrichment [22, 32, 36, 37].

With increasing drainage time, the concentrations of K^+, Na^+, Ca^{2+}, Mg^{2+}, Cl^-, and SO_4^{2-} in the water samples decreased with the gradual discharge of fracturing fluid. The decrease in Ca^{2+} and Mg^{2+} concentrations also indicated that the water-rock interactions had weakened (Figures 2(a)–2(f)). Water-rock interactions were affected by the rainy season in August; the latter strengthened them such that Ca^{2+} and Mg^{2+} concentrations increased and the Ca^{2+} concentration increased significantly (Figures 2(c) and 2(d)). As the dissolution rate of calcite is much higher than that of dolomite, the Ca^{2+} concentration in water was generally higher than the Mg^{2+} concentrations. SO_4^{2-} accumulations are primarily related to the dissolution and desulfurization of gypsum [38]. In a reducing environment, sulfate in coal seam

Table 2: Conventional ion data and hydrogen and oxygen isotope data from water samples.

CBM wells	Date	K^+ mg/L	Na^+ mg/L	Ca^{2+} mg/L	Mg^{2+} mg/L	Cl^- mg/L	SO_4^{2-} mg/L	HCO_3^- mg/L	$\delta^{13}C_{DIC}$ ‰V-PDB	$\delta^{18}O$ ‰V-SMOW	δD ‰V-SMOW
L-1	Apr. 2018	391.24	2337.93	22.77	9.62	3693.08	40.27	756.37	-5.11	-9.82	-58.54
	May 2018	388.14	2841.09	21.73	11.96	3566.23	22.89	899.61	-5.21	-10.09	-72.55
	Jun. 2018	448.06	2507	5.79	11.28	3622.01	19.57	1085.56	-5.12	-10.5	-70.69
	Jul. 2018	430.12	2393.63	19.22	9.48	3192	15.89	1483.55	-5.39	-10.42	-68.35
	Aug. 2018	271.02	2127.24	15.31	7.69	2841.46	17.33	1687	-4.67	-10.71	-71.73
	Sep. 2018	160.01	2006.09	12.35	5.08	2242.71	12.93	1830.97	-4.57	-11.03	-72.2
	Oct. 2018	153.98	1927.91	9.55	4.49	2083.21	8.47	1896.7	-4.25	-11.26	-74.51
	Nov. 2018	148.36	1966.38	8.14	4.63	1955.64	8.89	1931.12	-4.36	-11.38	-81.57
	Mean	298.87	2263.41	14.36	8.03	2899.54	18.28	1446.36	-4.84	-10.65	-71.27
L-2	Apr. 2018	653.81	3022.21	33.37	12.4	4742.68	34.82	1389.61	-7.96	-10.47	-72.97
	May 2018	413.98	2979.6	22.48	8.59	3392.58	24.2	1683.62	-8.13	-10.98	-82.04
	Jun. 2018	360.69	2711.59	18.91	7.73	2941.82	24.38	1826.85	-8.02	-11.68	-80.69
	Jul. 2018	298.37	2416.54	16.39	6.57	2539.78	19.89	2400.6	-8.19	-11.11	-76.28
	Aug. 2018	233.85	2202.94	17.2	5.54	2112.89	17.87	2519.54	-7.91	-11.76	-82.18
	Sep. 2018	242.97	2191.07	12.93	4.85	2315.7	14.61	2463.2	-8.23	-11.9	-83.77
	Oct. 2018	223.84	2121.72	10.76	4.42	2197.32	11.88	2475.72	-8.45	-11.76	-81.82
	Nov. 2018	220.1	2238.44	9.63	4.61	2101.83	10.3	2516.41	-8.50	-12.06	-86.66
	Mean	330.95	2485.51	17.71	6.84	2793.08	19.74	2159.44	-8.17	-11.46	-80.80
L-3	May 2018	253.39	2192.75	29.47	9.42	2953.54	19.78	562.88	-8.43	-11.38	-84.88
	Jun. 2018	179.97	1635.28	18.14	6.30	2072.06	22.75	731.24	-8.64	-12.30	-84.57
	Jul. 2018	133.49	1328.21	12.14	4.29	1560.49	17.57	895.14	-9.01	-11.38	-78.95
	Aug. 2018	97.87	1045.43	12.68	2.84	1203.64	15.36	960.87	-8.49	-12.36	-86.08
	Sep. 2018	75.52	865.79	7.19	2.17	983.43	13.21	1042.24	-8.32	-12.29	-85.39
	Oct. 2018	66.06	909.12	6.23	1.80	822.17	11.34	1032.85	-8.29	-12.51	-86.65
	Nov. 2018	51.37	827.43	4.61	1.20	604.21	9.03	1070.41	-8.36	-10.94	-78.20
	Mean	122.52	1257.72	12.92	4.00	1457.08	15.58	899.38	-8.51	-11.88	-83.53
L-4	May 2018	362.71	3228.39	19.29	9.29	3436.52	0.37	2168.6	-5.18	-11.59	-78.69
	Jun. 2018	330.54	3123.74	14.79	8.89	3235.61	0.19	2291.73	-5.12	-11.76	-79.1
	Jul. 2018	276.25	2883.28	20.35	7.92	2813.12	0.20	2967.11	-5.12	-11.09	-74.36
	Aug. 2018	235.56	2734.76	22.92	7.11	2702.08	0.32	3045.35	-4.13	-11.89	-78.54
	Sep. 2018	206.35	2564.84	17.49	5.46	2454.66	0.46	3170.55	-4.11	-11.69	-79.46
	Oct. 2018	200.69	2565.69	17.31	5.60	2358.30	0.42	3233.15	-4.18	-11.72	-79.57
	Nov. 2018	207.43	2564.53	16.43	5.96	2255.89	0.30	3358.34	-4.38	-11.82	-83.97
	Mean	259.93	2809.32	18.37	7.18	2750.88	0.32	2890.69	-4.60	-11.65	-79.10
L-5	May 2018	348.91	2609.78	9.92	7.31	2637.24	3.87	1084.65	-6.42	-11.95	-82.34
	Jun. 2018	227.40	2270.35	10.42	5.70	2302.85	0.05	956.49	-6.39	-12.11	-82.41
	Jul. 2018	174.65	2077.51	11.55	4.81	1995.86	3.88	1325.18	-6.76	-11.37	-77.65
	Aug. 2018	150.75	1867.78	15.81	4.42	1811.29	4.24	1425.33	-6.15	-11.49	-81.43
	Sep. 2018	136.65	1766.55	9.44	3.36	1554.92	3.33	1522.36	-6.06	-12.03	-83.38
	Oct. 2018	116.04	1757.51	7.66	3.00	1422.65	0.09	1525.49	-5.97	-12.01	-82.06
	Nov. 2018	114.00	1746.44	7.30	3.04	1345.38	0.96	1569.30	-6.02	-10.28	-80.61
	Mean	181.20	2013.70	10.30	4.52	1867.17	2.35	1344.11	-6.25	-11.61	-81.41

Table 2: Continued.

CBM wells	Date	K^+ mg/L	Na^+ mg/L	Ca^{2+} mg/L	Mg^{2+} mg/L	Cl^- mg/L	SO_4^{2-} mg/L	HCO_3^- mg/L	$\delta^{13}C_{DIC}$ ‰V-PDB	$\delta^{18}O$ ‰V-SMOW	δD ‰V-SMOW
L-6	May 2018	348.91	2609.78	9.92	7.31	2637.24	3.87	1884.65	-4.93	-11.95	-82.34
	Jun. 2018	299.72	2501.88	7.52	6.54	2525.99	1.61	1939.93	-5.53	-11.92	-82.2
	Jul. 2018	259.45	2316.31	11.08	6.55	2383.26	1.13	2381.82	-5.52	-11.25	-77.2
	Aug. 2018	213.25	2093.49	15.42	5.5	2171.06	0.29	2488.24	-4.84	-12.12	-81.7
	Sep. 2018	197.32	2006.94	11.07	4.38	1910.23	0.74	2600.91	-4.79	-12.03	-83.96
	Oct. 2018	207.93	2011.09	10.51	4.44	1803.25	0.09	2660.38	-4.36	-12.06	-83.23
	Nov. 2018	181.62	2060.99	9.48	4.42	1649.12	0.13	2760.54	-4.43	-11.52	-84.52
	Mean	244.03	2228.64	10.71	5.59	2154.31	1.12	2388.07	-4.91	-11.84	-82.16

water can produce bicarbonate and H_2S gas with organic matter, showing HCO_3^- concentrations increasing with time and SO_4^{2-} concentrations decreasing with time (Figures 2(f) and 2(g)).

According to this analysis, the groundwater hydrological environment in the study area is, overall, in a closed state with poor hydrodynamic conditions. Na^+, K^+, Cl^-, and HCO_3^- concentrations in this study were enriched in the confined groundwater environment, and Na^+, K^+, and Cl^- were present in the fracturing fluid, so HCO_3^- was chosen as the ion with which to study gas productivity response. Figure 3 shows that there was a positive correlation between HCO_3^- and CBM production in the produced water. Among these wells, L-4 and L-6 had the highest HCO_3^- concentration; their gas production is also the highest.

3.2. Hydrogen and Oxygen Isotope Characteristics and Productivity Response. When the isotope value of produced water is located on the left side of the atmospheric precipitation line, it shows a D drift characteristic; when the value is on the right side, it shows an O drift characteristic. Except for the O drift characteristic in May and November, the produced water in well L-1 showed a D drift characteristic. For produced water of well L-4, they all show an O drift characteristic except for July and August. The values of well L-6 also exhibited an O drift characteristic except for August. As for wells L-2, L-3, and L-5, they all showed an O drift characteristic (Figure 4).

The isotope values of δD and $\delta^{18}O$ in the produced water are negatively correlated with drainage time; however, the δD and $\delta^{18}O$ isotope values suddenly increased in July (Figures 5(a) and 5(b)). The δD isotope value in the produced water of well L-3 suddenly increased in November (Figure 5(a)), and the $\delta^{18}O$ isotope value in the produced water in wells L-3, L-5, and L-6 increased suddenly in November (Figure 5(b)).

Our quantification of the hydrogen and oxygen isotopic composition is based on the Yunnan atmospheric precipitation line equation $\delta D = 6.56\delta^{18}O - 2.96$ [39]. When groundwater flows through coal-bearing strata, several hydrogen-bearing soluble minerals in the coal seams are dissolved continuously. The lighter H atoms in hydrogen-bearing minerals are easily adsorbed by minerals such as clay, while the heavier D atoms are more likely to undergo an isotope exchange with H atoms in the water, thereby continuously enriching D in the formation water and exhibiting D drift characteristics [22, 26]. ^{18}O is enriched in the surrounding rock. With groundwater runoff, many oxygen-bearing soluble minerals in the formation are dissolved continuously. The heavier ^{18}O in the mineral is liable to undergoing isotope exchange reaction with the lighter ^{16}O in the groundwater and thus to show ^{18}O drift characteristics [22, 40].

Hydrogen and oxygen isotopes of produced water analyzed in this study are distributed near the atmospheric precipitation line, showing obvious D drift characteristics; a few have ^{18}O drift characteristics because of atmospheric precipitation or weak mixing with the surface water and shallow groundwater [41, 42].

With the drainage of CBM wells, the water-rock interactions between the fracturing fluids remaining in the coal seam or formation water and the coal seam or surrounding rocks gradually weakened. However, July and August are rainy seasons in Yunnan and result in strong recharge from atmospheric precipitation. Therefore, the variation in the δD and $\delta^{18}O$ isotope values in July may have been caused by seasonal rainfall. Studies of δD and $\delta^{18}O$ isotopes in produced water from the six wells show that these changes are universal (Figures 5(a) and 5(b)). The δD and $\delta^{18}O$ isotope values from produced water in well L-3 increased sharply in November; this was also true of the $\delta^{18}O$ isotope value for well L-5, although its δD isotope value increased only slightly in November; these results are different from those of the other four wells (Figures 5(a) and 5(b)). The drift characteristics of wells L-1 and L-2 are presumed to be caused by the fragmentation of the water-bearing limestone on the top of the coal seam. Combined with the enrichment mechanism of D and ^{18}O [22, 26, 40], it was inferred that the trend of wells L-4 and L-6 is conducive to the long-term production of CBM; the actual gas production situation also verified this inference (Figure 6). Anomalies (reservoir damage or wellbore collapse) were observed for the remaining four wells, although wells L-1 and L-2 had high gas production; however, the former conditions are not conducive to the long-term production of CBM.

3.3. Dissolved Inorganic Carbon Characteristics and Productivity Response. The $\delta^{13}C_{DIC}$ values of the water samples from the produced water were not significantly different, and the change trends were similar: generally falling initially, subsequently rising, and then falling again. Wells L-1, L-4, L-

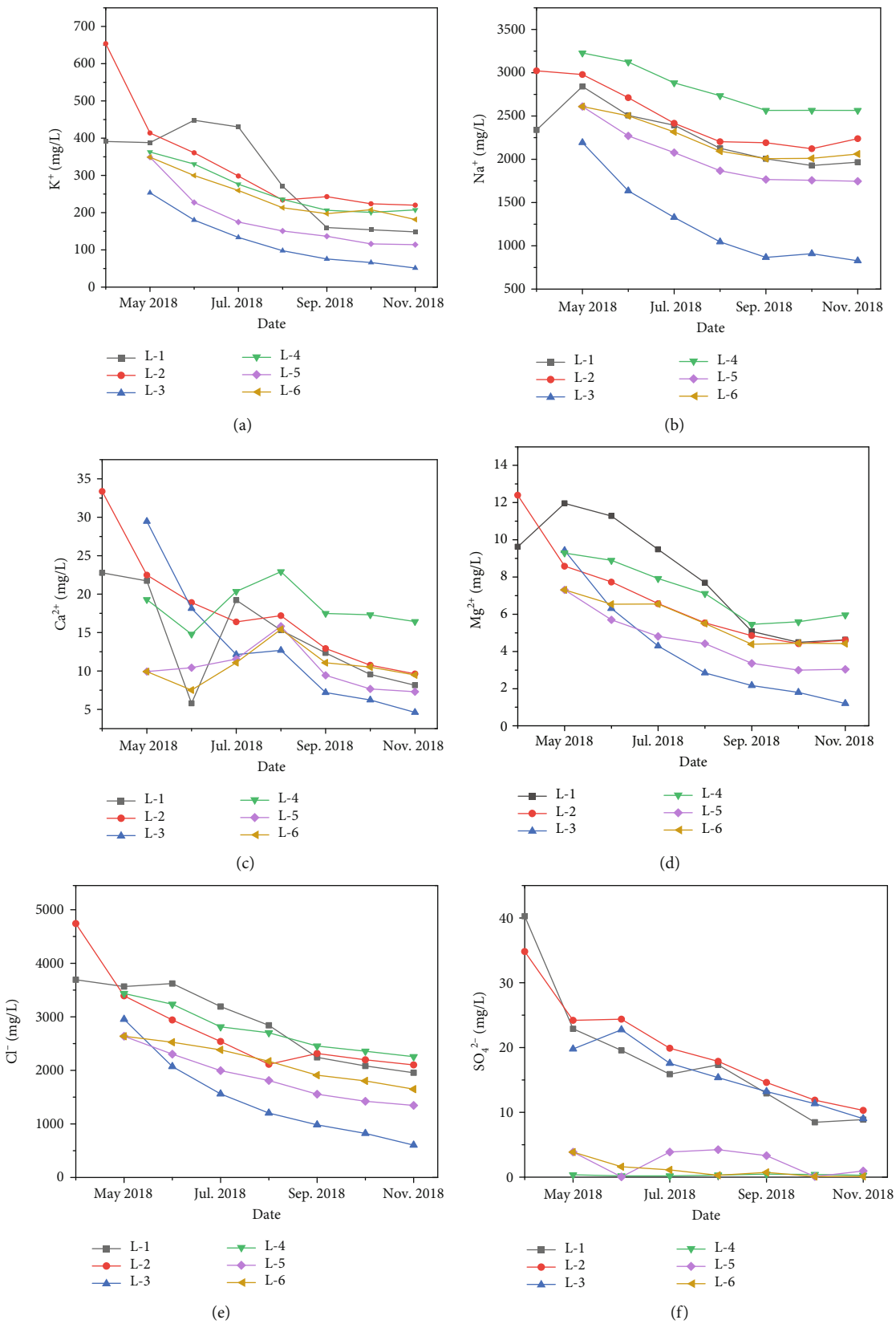

Figure 2: Continued.

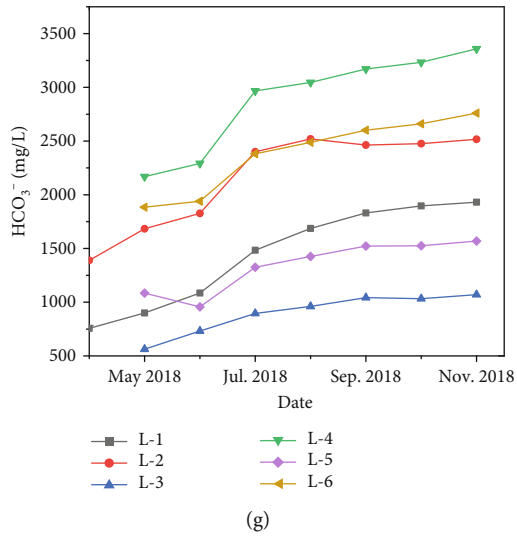

(g)

Figure 2: Ion concentration changes with time.

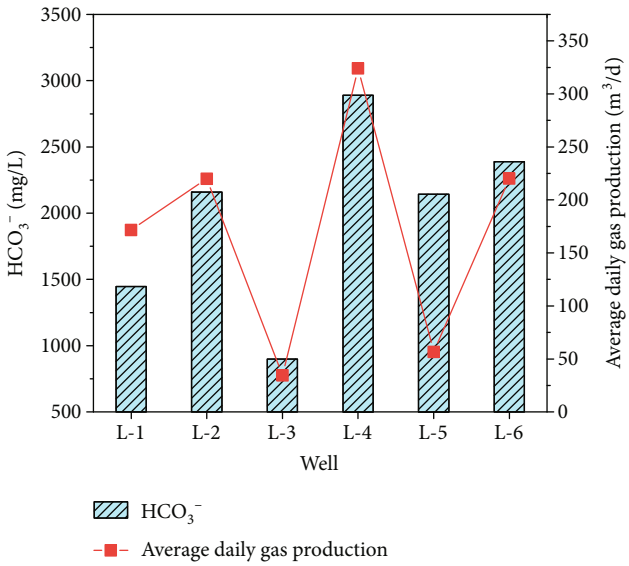

Figure 3: The relationship between HCO_3^- and gas production.

5, and L-6 had the highest $\delta^{13}C_{DIC}$ values, the surface water samples had the lowest $\delta^{13}C_{DIC}$ values, and wells L-2 and L-3 had $\delta^{13}C_{DIC}$ values between the two extremes (Figure 7).

The composition of $^{13}C_{DIC}$ from different sources was significantly different, appearing primarily in the forms of H_2CO_3, HCO_3^-, CO_3^{2-}, and water-soluble CO_2. $\delta^{13}C_{DIC}$ values based on organic origins are less than -8‰, and those formed by inorganic origin are approximately 0‰ [27, 29, 43].

The two sources of $\delta^{13}C_{DIC}$ in surface and shallow water are primarily related to oxidation via the CO_2 produced by plant respiration and decomposition and the dissolution of carbonate rocks in soil. Carbon dioxide dissolves in water and continuously exchanges carbon isotopes with H_2CO_3, HCO_3^-, and CO_3^{2-} in water, reducing the value of $\delta^{13}C_{DIC}$ in groundwater. If the concentration of HCO_3^- in the water is high, the value of $\delta^{13}C_{DIC}$ will be low. The $\delta^{13}C_{DIC}$ value of surface and shallow water is usually between -14‰ and -7‰, falling into the range of extremely low negative values [35, 44].

The isotope $^{13}C_{DIC}$ is abundant in produced water of CBM wells and primarily derived from carbonate mineral dissolution and microbial methanogenesis [34]. Methanogenesis in the study area is weak; therefore, the observed change in $^{13}C_{DIC}$ content is controlled mostly by the dissolution of carbonate minerals. Carbonate minerals in coal measure strata are more abundant than ^{13}C in soil carbonates. When they dissolve, the $\delta^{13}C_{DIC}$ value in water increases and ranges from -7‰ to 0‰ [45].

The $\delta^{13}C_{DIC}$ value of surface water samples is in an extremely low negative value range. This is likely a result of atmospheric CO_2 dissolution, plant respiration, and the dissolution of carbonate rocks in the soil (Figure 7). An analysis of the relationship between $\delta^{13}C_{DIC}$ values and their source characteristics shows that the produced water samples can be divided into two categories: (1) water samples from wells L-2 and L-3, with $\delta^{13}C_{DIC}$ values ranging from -9‰ to -7‰, which is consistent with shallow water and due primarily to the process of atmospheric CO_2 dissolution, plant respiration, and the dissolution of carbonate rocks in soil; (2) water samples from wells L-1, L-4, L-5, and L-6, with $\delta^{13}C_{DIC}$ values ranging from -6.3‰ to -4‰. The burial depth of the coal seam is approximately 750 m, and the concentration of HCO_3^- is high, mainly because the carbonate minerals in the coal are dissolved. The $\delta^{13}C_{DIC}$ values of produced water are positively correlated with gas production (except for well L-2, which may have been caused by a precipitation injection during the rainy season) (Figure 8). When $^{13}C_{DIC}$ in the produced water is the carbonate mineral dissolved in coal seam water, the gas production is high.

4. Conclusions

Based on an analysis of the time-varying characteristics of conventional ions, hydrogen and oxygen isotopes, and DIC

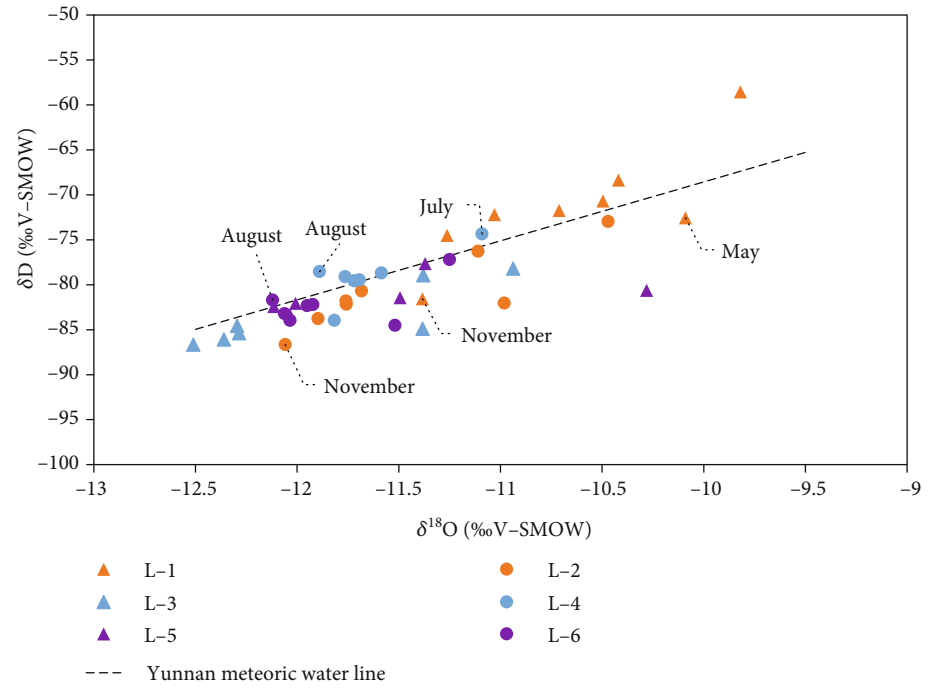

Figure 4: Relationship between δD and δ^{18}O isotopes in produced water.

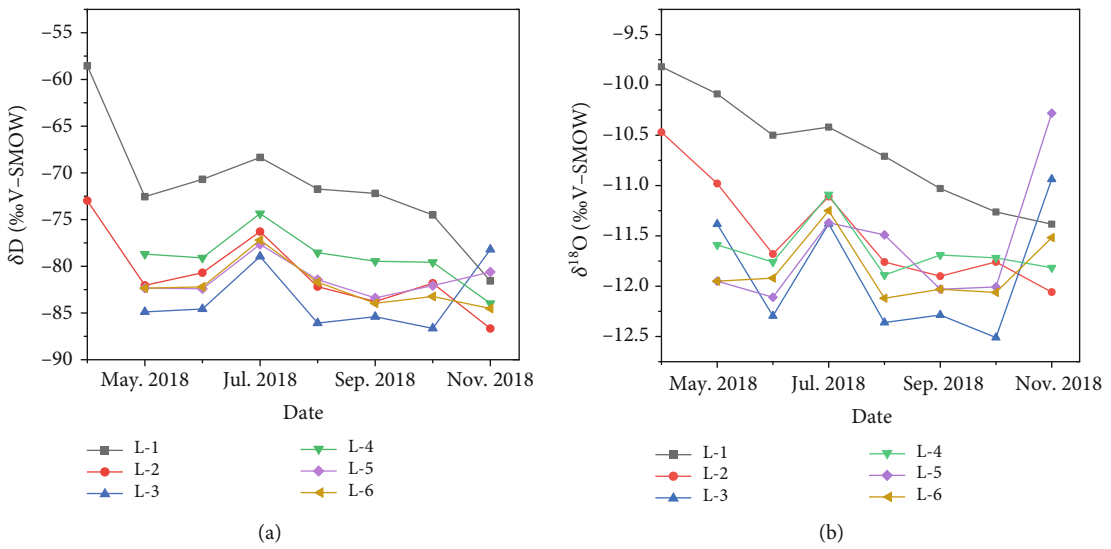

Figure 5: Variation of D and ^{18}O isotopes in production water with time.

content in the produced water from CBM wells in eastern Yunnan, the following conclusions were obtained:

(1) The produced water type of well L-3 is mainly Na-HCO_3, while those of the other five wells are Na-Cl-HCO_3. The cations in the produced water are mainly K^+, Na^+, Ca^{2+}, and Mg^{2+}. The changes in concentration are characterized by fluctuations that are primarily affected by water-rock interactions. The anions are mostly Cl^- and HCO_3^-, and the value of the former shows a decreasing trend related to the continuous discharge of the fracturing fluid while the latter shows an increasing trend related to the dissolution of carbonate minerals in coal. The concentration of HCO_3^- in produced water is positively correlated with CBM production

(2) The hydrogen and oxygen isotopes in the produced water of the study area are distributed near the regional atmospheric precipitation line, showing D drift or O drift characteristics that indicate that the produced water is greatly affected by water-rock

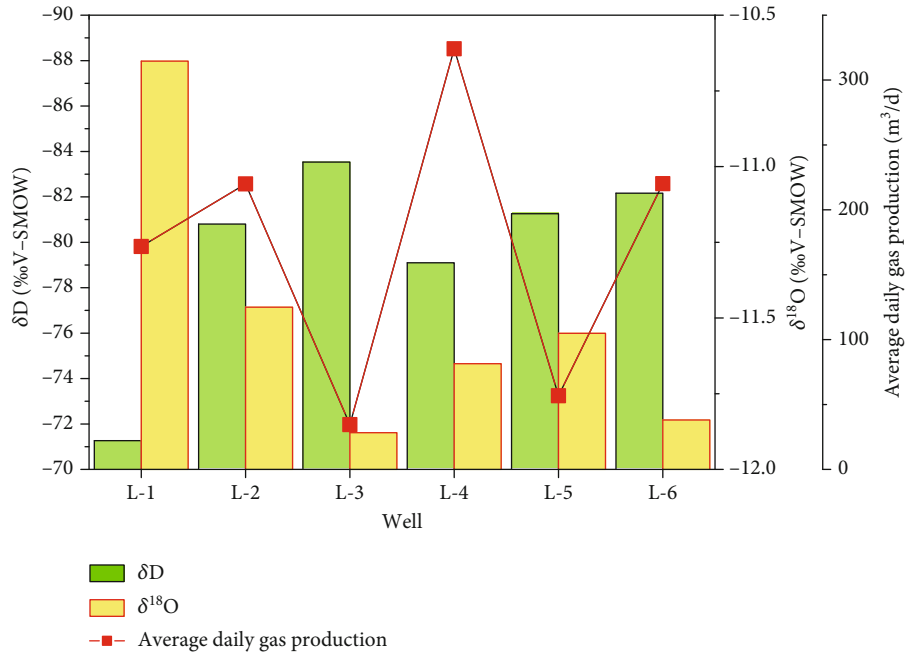

Figure 6: The relationship between δD and $\delta^{18}O$ isotopes and gas production in produced water.

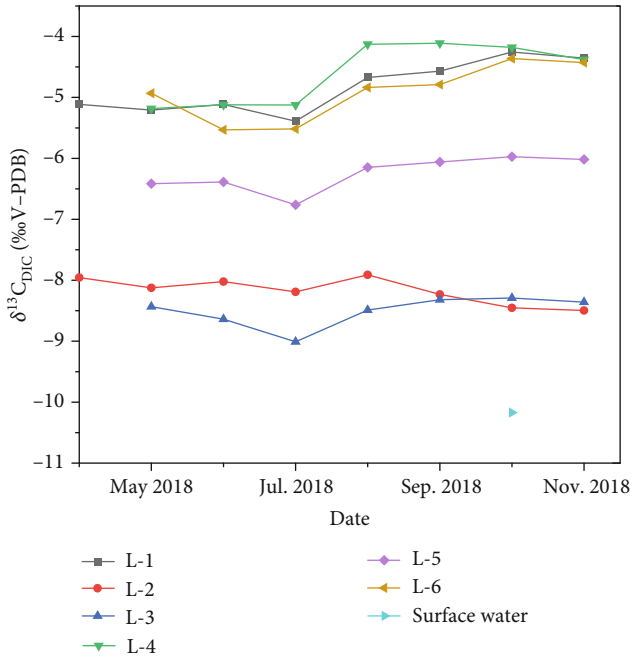

Figure 7: Variation of dissolved inorganic carbon in production water with time.

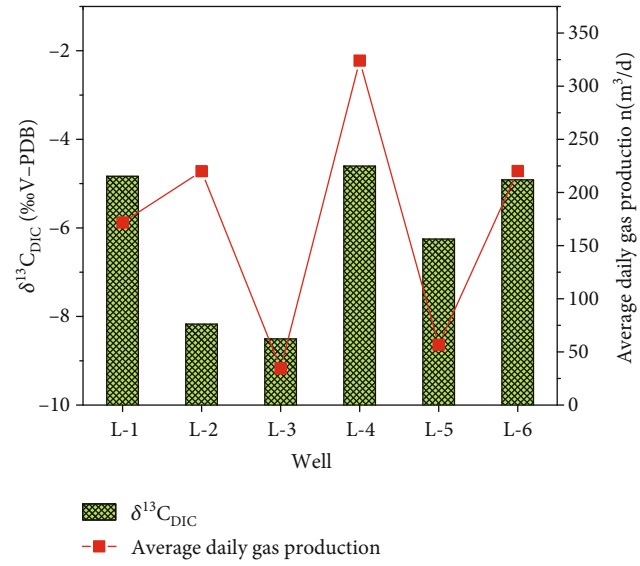

Figure 8: Relationship between dissolved inorganic carbon isotopes and gas production.

interactions. This, combined with the enrichment mechanism of D and ^{18}O, suggests that D drift is beneficial to the production of CBM. Water samples from wells L-2 and L-3 are primarily derived from the atmospheric CO_2 dissolution, plant respiration, and carbonate dissolution in the soil. Water samples from wells L-1, L-4, L-5, and L-6 are primarily derived from the carbonate mineral dissolved in coal seam water. When the $^{13}C_{DIC}$ is from the carbonate minerals dissolved in coal seam water, gas production is high. Wells L-4 and L-6 produce the most gas due to having the highest concentrations of HCO_3^- in produced water, D drift characteristics, and $^{13}C_{DIC}$ derived from the dissolution of carbonate minerals in coal

Data Availability

The data used to support the findings of this study are included within the article.

Conflicts of Interest

The authors declare that they have no conflicts of interest.

Acknowledgments

This work was supported by the National Natural Science Foundation of China (nos. 41572140 and 41872170), the National Major Special Project of Science and Technology of China (no. 2016ZX05044001), the National Natural Science Foundation Project (no. 41802181), the Natural Science Foundation Project of Jiangsu Province (no. BK20180660), and the Qing Lan Project.

References

[1] I. Hamawand, T. Yusaf, and S. G. Hamawand, "Coal seam gas and associated water: a review paper," *Renewable and Sustainable Energy Reviews*, vol. 22, pp. 550–560, 2013.

[2] K. G. Dahm, K. L. Guerra, P. Xu, and J. E. Drewes, "Composite geochemical database for coalbed methane produced water quality in the Rocky Mountain Region," *Environmental Science and Technology*, vol. 45, no. 18, pp. 7655–7663, 2011.

[3] Z. Zhang and Y. Qin, "A preliminary investigation on water quality of coalbed natural gas produced water for beneficial uses: a case study in the Southern Qinshui Basin, North China," *Environmental Science and Pollution Research*, vol. 25, no. 22, pp. 21589–21604, 2018.

[4] Z. B. Yang, Y. Qin, C. C. Wu, Z. H. Qin, G. Li, and C. L. Li, "Geochemical response of produced water in the CBM well group with multiple coal seams and its geological significance-a case study of the Songhe well group in Western Guizhou," *International Journal of Coal Geology*, vol. 207, pp. 39–51, 2019.

[5] J. P. Ye, Q. Wu, and Z. H. Wang, "Controlled characteristics of hydrogeological conditions on the coalbed methane migration and accumulation," *Journal of China Coal Society*, vol. 26, pp. 459–462, 2001.

[6] S. Bachu and K. Michael, "Possible controls of hydrogeological and stress regimes on the producibility of coalbed methane in Upper Cretaceous-Tertiary strata of the Alberta basin, Canada," *AAPG Bulletin*, vol. 87, no. 11, pp. 1729–1754, 2003.

[7] J. C. Pashin, M. R. Mcintyre-Redden, S. D. Mann, D. C. Kopaska-Merkel, M. Varonka, and W. Orem, "Relationships between water and gas chemistry in mature coalbed methane reservoirs of the Black Warrior Basin," *International Journal of Coal Geology*, vol. 126, pp. 92–105, 2014.

[8] M. M. Wei and Y. W. Ju, "Chemical characteristics and origin of produced waters from coalbed gas field in the southern of Qinshui Basin," *Journal of China Coal Society*, vol. 40, pp. 629–635, 2015.

[9] X. Y. Zhang, C. F. Wu, and S. X. Liu, "Characteristic analysis and fractal model of the gas-water relative permeability of coal under different confining pressures," *Journal of Petroleum Science and Engineering*, vol. 159, pp. 488–496, 2017.

[10] W. A. Van Voast, "Geochemical signature of formation waters associated with coalbed methane," *AAPG Bulletin*, vol. 87, no. 4, pp. 667–676, 2003.

[11] M. Taulis and M. Milke, "Chemical variability of groundwater samples collected from a coal seam gas exploration well, Maramarua, New Zealand," *Water Research*, vol. 47, no. 3, pp. 1021–1034, 2013.

[12] C. F. Wu, S. Yao, and Y. F. Du, "Production systems optimization of a CBM well based on a time series BP neural network," *Journal of China University of Mining and Technology*, vol. 44, pp. 64–69, 2015.

[13] S. Tao, Z. J. Pan, S. D. Chen, and S. L. Tang, "Coal seam porosity and fracture heterogeneity of marcolithotypes in the Fanzhuang Block, southern Qinshui Basin, China," *Journal of Natural Gas Science and Engineering*, vol. 66, pp. 148–158, 2019.

[14] B. Y. Zhou, Y. Qin, and Z. B. Yang, "Ion composition of produced water from coalbed methane wells in western Guizhou, China, and associated productivity response," *Fuel*, vol. 265, article 116939, 2020.

[15] M. Yang, Y. W. Ju, G. J. Liu, L. Tong, Y. Kang, and Q. L. Hou, "Geochemical characters of water coproduced with coalbed gas and shallow groundwater in Liulin Coalfield of China," *Acta Geologica Sinica*, vol. 87, no. 6, pp. 1690–1700, 2013.

[16] S. H. Zhang, S. H. Tang, Z. C. Li, Z. J. Pan, and W. Shi, "Study of hydrochemical characteristics of CBM co-produced water of the Shizhuangnan Block in the southern Qinshui Basin, China, on its implication of CBM development," *International Journal of Coal Geology*, vol. 159, pp. 169–182, 2016.

[17] C. Li, S. H. Tang, S. H. Zhang, S. B. Wang, and Z. Li, "Chemical characteristics and significance of CBM well produced water in Shizhuang South Area, Qinshui Basin," *Coal Geology of China*, vol. 25, pp. 25–29, 2013.

[18] H. Z. Huang, S. X. Sang, Y. Miao, Z. T. Dong, and H. J. Zhang, "Trends of ionic concentration variations in water coproduced with coalbed methane in the Tiefa Basin," *International Journal of Coal Geology*, vol. 182, pp. 32–41, 2017.

[19] S. Tao, Z. J. Pan, S. L. Tang, and S. D. Chen, "Current status and geological conditions for the applicability of CBM drilling technologies in China: A review," *International Journal of Coal Geology*, vol. 202, pp. 95–108, 2019.

[20] Z. Zhang, D. T. Yan, X. G. Zhuang et al., "Hydrogeochemistry signatures of produced waters associated with coalbed methane production in the Southern Junggar Basin, NW China," *Environmental Science and Pollution Research*, vol. 26, no. 31, pp. 31956–31980, 2019.

[21] Z. Zhang, Y. Qin, J. P. Bai, G. Q. Li, X. G. Zhuang, and X. M. Wang, "Hydrogeochemistry characteristics of produced waters from CBM wells in Southern Qinshui Basin and implications for CBM commingled development," *Journal of Natural Gas Science and Engineering*, vol. 56, pp. 428–443, 2018.

[22] C. C. Wu, Z. B. Yang, Y. Qin, J. Chen, Z. G. Zhang, and Y. Y. Li, "Characteristics of hydrogen and oxygen isotopes in produced water and productivity response of coalbed methane wells in Western Guizhou," *Energy & Fuels*, vol. 32, no. 11, pp. 11203–11211, 2018.

[23] Z. B. Yang, C. C. Wu, Z. G. Zhang, J. Jin, L. Y. Zhao, and Y. Y. Li, "Geochemical significance of CBM produced water: a case study of developed test wells in Songhe block of Guizhou province," *Journal of China University of Mining and Technology*, vol. 46, pp. 710–717, 2017.

[24] G. T. Snyder, W. C. Riese, S. Franks et al., "Origin and history of waters associated with coalbed methane: ^{129}I, ^{36}Cl, and stable isotope results from the Fruitland Formation, CO and NM," *Geochimica et Cosmochimica Acta*, vol. 67, no. 23, pp. 4529–4544, 2003.

[25] J. X. Dai, J. Li, X. Luo et al., "Stable carbon isotope compositions and source rock geochemistry of the giant gas accumulations in the Ordos Basin, China," *Organic Geochemistry*, vol. 36, no. 12, pp. 1617–1635, 2005.

[26] C. A. Rice, R. M. Flores, G. D. Stricker, and M. S. Ellis, "Chemical and stable isotopic evidence for water/rock interaction and biogenic origin of coalbed methane, Fort Union Formation, Powder River Basin, Wyoming and Montana U.S.A.," *International Journal of Coal Geology*, vol. 76, no. 1-2, pp. 76–85, 2008.

[27] A. M. Aucour, R. Bonnefille, and C. Hillairemarcel, "Sources and accumulation rates of organic carbon in an equatorial peat bog (Burundi, East Africa) during the Holocene: carbon isotope constraints," *Palaeogeography Palaeoclimatology Palaeoecology*, vol. 51, pp. 179–189, 1999.

[28] J. X. Dai, X. Shi, and Y. Z. Wei, "Summary of the abiogenic origin theory and the abiogenic gas pools (fields)," *Acta Petrolei Sinica*, vol. 22, pp. 5–10, 2001.

[29] K. Rive, P. Agrinier, and J. Gaillardet, *DIC dynamics in stream water of volcanic settings: climatic and lithology impact on the CO_2 chemical weathering (Lesser Antilles, Reunion, French Massif Central and Iceland)*, AGU Fall Meeting Abstracts, 2006.

[30] Z. C. Li, S. H. Tang, X. F. Wang et al., "Relationship between water chemical composition and production of coalbed methane wells, Qinshui basin," *Journal of China University of Mining and Technology*, vol. 40, pp. 424–429, 2011.

[31] B. S. Yu, "Chemical characteristic of produced water of Jun Lian CBM well and its intention," *China Coalbed Methane*, vol. 12, pp. 32–35, 2015.

[32] C. Guo, Y. Qin, Y. C. Xia et al., "Geochemical characteristics of water produced from CBM wells and implications for commingling CBM production: a case study of the Bide-Santang Basin, western Guizhou, China," *Journal of Petroleum Science and Engineering*, vol. 159, pp. 666–678, 2017.

[33] T. A. Moore, "Coalbed methane: a review," *International Journal of Coal Geology*, vol. 101, pp. 36–81, 2012.

[34] T. G. Lemay and K. O. Konhauser, *Water chemistry of coalbed methane reservoirs*, Alberta Energy and Utilities Board, 2006, EUB/AGS, Special Report.

[35] S. A. Quillinan and C. D. Frost, "Carbon isotope characterization of powder river basin coal bed waters: key to minimizing unnecessary water production and implications for exploration and production of biogenic gas," *International Journal of Coal Geology*, vol. 126, pp. 106–119, 2014.

[36] C. Guo, Y. Qin, D. M. Ma et al., "Ionic composition, geological signature and environmental impacts of coalbed methane produced water in China," *Energy Sources, Part A: Recovery, Utilization, and Environmental Effects*, pp. 1–15, 2019.

[37] C. Guo, Y. Qin, and D. Han, "Interlayer interference analysis based on trace elements in water produced from coalbed methane wells: a case study of the Upper Permian coal-bearing strata, Bide–Santang Basin, western Guizhou, China," *Arabian Journal of Geosciences*, vol. 10, no. 6, 2017.

[38] P. Birkle and J. J. Rosillo Aragon, "Evolution and orgin of deep reservoir water at the Activo Luna oil field, Gulf of Mexico, Mexico," *AAPG Bulletin*, vol. 86, pp. 457–484, 2002.

[39] H. Hu and J. L. Wang, "On characteristics of hydrogen and oxygen isotope in precipitation in Yunnan and analysis of moisture sources," *Journal of Southwest China Normal University (Natural Science Edition)*, vol. 40, pp. 142–149, 2015.

[40] L. W. Chen, H. R. Gui, X. X. Yin, and J. Z. Qian, "Composing characteristic of ^{18}O and D and current field in deep groundwater," *Journal of China University of Mining and Technology*, vol. 37, pp. 854–859, 2008.

[41] W. Dansgaard, "Stable isotopes in precipitation," *Tellus*, vol. 16, pp. 436–468, 1964.

[42] Q. Y. Mao, J. L. Wang, J. L. Wang, and W. Li, "Analysis of the characteristics of δD and $\delta^{18}O$ in the meteoric precipitation in Anshun, Guizhou Province and Beibei Chongqing," *Journal of Southwest University (Natural Science Edition)*, vol. 39, pp. 114–120, 2017.

[43] E. L. Brinck, J. I. Drever, and C. D. Frost, "The geochemical evolution of water coproduced with coalbed natural gas in the Powder River Basin, Wyoming," *Environmental Geosciences*, vol. 15, no. 4, pp. 153–171, 2008.

[44] J. F. McLaughlin, C. D. Frost, and S. Sharma, "Geochemical analysis of Atlantic Rim water, Carbon County, Wyoming: new applications for characterizing coalbed natural gas reservoirs," *AAPG Bulletin*, vol. 95, no. 2, pp. 191–217, 2011.

[45] L. W. Chen, H. R. Gui, and X. X. Yin, "Composing characteristic and evolution law of carbon and oxygen stable isotopes in groundwater dissolved carbonate," *Journal of China Coal Society*, vol. 33, pp. 537–542, 2008.